

Article

# Biosensor-based strategies for promoting innovation and assessing occupational health risks among college students

Fang Li

Wuhan Business University, Wuhan 430056, China; [li\\_fang02@163.com](mailto:li_fang02@163.com)

## CITATION

Li F. Biosensor-based strategies for promoting innovation and assessing occupational health risks among college students. *Molecular & Cellular Biomechanics*. 2024; 21(4): 820.  
<https://doi.org/10.62617/mcb820>

## ARTICLE INFO

Received: 18 November 2024  
Accepted: 2 December 2024  
Available online: 20 December 2024

## COPYRIGHT



Copyright © 2024 by author(s).  
*Molecular & Cellular Biomechanics* is published by Sin-Chn Scientific Press Pte. Ltd. This work is licensed under the Creative Commons Attribution (CC BY) license.  
<https://creativecommons.org/licenses/by/4.0/>

**Abstract:** Higher education was increasingly emphasizing innovation and entrepreneurship strategy, encouraging college students to develop creative talents. The intense needs of both academic and entrepreneurial tasks provide serious occupational health hazards that affect students' physical and emotional health. This paper provides a novel approach to risk assessment and management that combines biosensor technology and artificial intelligence (AI). The emphasis is on applying a novel Flower Pollination Optimizer Tuned Gate refined Long Short Term Memory (FPO-GLSTM) method to monitor and forecast health issues, such as stress, physical strain, and other risk factors in education and entrepreneurship situations. Data were gathered using biosensors that monitored physiological characteristics, such as heart rate, blood pressure, and stress levels in real-time. To capture crucial health information, the data was pre-processed with min-max normalization, and features were extracted using the Discrete Wavelet Transform (DWT). The FPO-GLSTM model to forecast potential health hazards and make individualized recommendations. The outcomes demonstrate that the FPO-GLSTM-based model accurately and precisely forecasts health risks, including stress-induced conditions. AI and biosensor data integration offer a viable way to monitor and manage health risks for students, improving their health in educational and entrepreneurial environments.

**Keywords:** college students; health hazards; entrepreneurship; biosensor; Flower Pollination Optimizer Tuned Gate refined Long Short Term Memory (FPO-GLSTM)

## 1. Introduction

Today's education professionals must possess the information, abilities, and skills necessary to strategize the problems that engineering students face. Examining a new approach is necessary to find an appropriate solution for the course curriculum and results in light of the integration of evolving trends, technology, and student demands. To accomplish educational renovation, the traditional teaching style must be drastically altered [1]. Students will benefit from this educational innovation by developing their creativity to discover novel approaches and fresh problem-solving strategies through practical, real-time experiments and experiences. Its refurbishment is crucial to closing the gap between the real issues and the teaching-learning process in the classroom. This kind of educational reform approach is beneficial for students to solve difficulties in real time [2]. The major components that provide data like temperature, pressure, electroencephalograms, and electromyograms are the biosensors; secondary components that link the biosensors and receiving apparatus, including indicating and recording devices, are the transducers [3]. Learning models, such as evaluation expectations, learning conceptions, and self-efficacy beliefs have a big influence on how students in higher education learn. As a result, promoting and supporting entrepreneurial environments in the context of entrepreneurship education

may benefit young adult learners preparing for a future as entrepreneurs [4]. Entrepreneurship is crucial for governments looking into the educational global economy, though it is frequently viewed as a way to promote economic growth, innovation, and inventiveness. The creation of educational programs that encourage and promote entrepreneurship is becoming more popular as a result of this perspective [5]. Risks associated with entrepreneurship techniques include competition, market volatility, financial instability, operational difficulties, and innovative failures. To reduce these risks and achieve long-term business growth and success, effective risk management, flexibility, and thorough investigation are important [6]. A large number of scholarships on the issue recognize the beneficial effects of entrepreneurship education on the growth of people's knowledge and skills as well as on the improvement of entrepreneurial attitude and intention, even though there is disagreement about whether or not learning, might promote entrepreneurship [7]. Students in non-business education programs are finding entrepreneurial abilities and one's own creative and knowledge-based thinking is becoming more and more important [8]. This is mostly due to a large percentage of graduates finding jobs in the business sector, either because of the challenging labor market in conventional life science industries or a lack of interest in long-term scientific employment [9]. Entrepreneurial employment is more demanding in terms of resources for well-being in addition to pressures. Entrepreneurs possess a level of freedom and autonomy that is difficult to find in other professions since entrepreneurship blends ownership and control [10]. The goal of the study is to offer a new method of risk assessment and management by fusing AI with biosensor technologies. The focus is on using new FPO-GLSTM techniques to track and predict health problems, including stress, physical strain, and other risk factors in contexts related to educational institutions and business enterprises.

#### Contribution of the research

The contributions are summarized below.

- Dataset is created from biosensor data that records physiological parameters in real-time, such as blood pressure, heart rate, and stress levels, and that represents health hazards in both academic and business contexts.
- The physiological data performed preprocessing using min-max normalization to ensure uniformity and remove discrepancies for accurate feature extraction and model performance.
- Important characteristics are extracted using the discrete wavelet transform (DWT), which indicates important patterns linked to physical strain and stress for predictive analysis.
- The proposed FPO-GLSTM model is innovative because it combines AI and biosensors to anticipate health concerns and deliver individualized suggestions to students.

The remainder of the document is structured as follows. The most significant related work is reviewed in Section 2, especially in the field of biosensors. Section 3 offers background information on fundamental concepts, especially DL-based biosensor assessment, and briefly discusses the entrepreneurship strategies that are used; the proposed biosensor will be presented. Section 4 initiates the evaluated health

risks, including stress-induced conditions performance. Section 5 Limitation and Future Work, along with a brief conclusion are presented.

## **2. Related work**

In recent years, various researchers have investigated biosensors in the context of entrepreneurial initiatives, notably in the ML and DL domains.

According to research [11], a unique assessment approach for analyzing students' learning about innovation and entrepreneurship using backpropagation (BP) neural networks was presented. It investigated the conceptual structure, elements, and development procedure of a BP neural network. They obtained outstanding results with careful training and analysis, with a maximum discrepancy of 1.6% between predicted and actual output.

In a study [12], an analytical approach utilizing artificial intelligence (AI), and big data for college students' employment and entrepreneurship was provided, to build a solid foundation for the growth of employment advising activities. The findings of the experiment showed that the method could handle and evaluate large textual datasets, resulting in improved data categorization outcomes.

Research [13] proposed to establish profiles of young Colombian entrepreneurs using data from the youth entrepreneurship study conducted by the Colombian youth secretariat. These findings identify key entrepreneurial skills, talents, and capacities, including innovation, learning, and leadership, and they further depict five profiles of entrepreneurs, mostly classified by age and entrepreneurship motivations.

A study [14] was focused on utilizing data from 25 top Higher Educational Institutions (HEI) across several provinces to create a new hybrid Machine Learning (ML) model that combines two potent methods, Logistic Regression (LR) and Random Forest (RF), to evaluate every level of innovation and entrepreneurship (I&E) in education. The study's findings showed that colleges have begun to integrate entrepreneurial skills into the curriculum, exhibited by a higher ranking on the issue of curricular development, followed by skill enrichment.

In the paper [15], the purpose of adopting this entrepreneurial-minded learning (EML) curriculum was to inspire first-year undergraduate chemistry students' inventiveness, creativity, and entrepreneurial learning. When they conducted course surveys to find out how students felt about this module, they found that most of them enjoyed the activity and gained practical skills.

Author [16] examined the factors influencing transformative entrepreneurship in digital platforms. It proposed a two-stage method. First, a model was proposed using interpretative structural modeling (ISM) and matrices impact crop multiplication applied to unclassement (MICMAC). ISM was a qualitative technique used to produce a visual hierarchy.

Research [17] used ML to assess the predictability of entrepreneurial activity. According to the data, the extreme gradient boosting (XG boost) tree ensemble forecasts this kind of entrepreneurial activity with 96.5% accuracy, outperforming all other methods.

The paper [18] enhanced research by incorporating educational theory and philosophy into higher education's entrepreneurial pedagogy and education. It

examined and highlighted the ways that constructivism, behaviorism, cognitivism, and humanism are applied to support and promote education in entrepreneurial institutions. To conceptualize how educational philosophies and concepts might be used in entrepreneurial education to benefit students.

The article [19] improved comprehension of the connections between academic achievement, study habits, perceptions of the learning environment, and sociodemographic characteristics of occupational therapy students. The student's academic success was not substantially impacted by the learning environment, despite the fact that maintaining a high standard of instruction is important for many reasons.

Work [20] provided deep neural networks (DNN) to final-year chemical engineering students through a computer laboratory activity. As part of a fast-track task, students were asked to create a DNN model and forecast the adsorption equilibrium of three distinct acids on activated carbon at four different temperatures.

A study [21] was essential in identifying the potential of social media platforms to support sustainable entrepreneurship in higher education as, despite their limited use, these channels might be used as an official source of data for education. Future research should investigate which types of material have the most effect on perceptions of sustainable entrepreneurship, as well as propose specific techniques for implementation in this field.

Research [22] aims to enhance the data development analysis-convolutional neural network (DEA-CNN) framework by evaluating the knowledge, abilities, and competencies of social entrepreneurs to create adaptable hybrid learning systems. In addition to addressing environmental problems, social entrepreneurship fosters cultural diversity. Many college students, especially those interested in business, value real action over mere ideas.

The framework [23] focused on practical application, directing curriculum creation to use AI technologies like ML and predictive analytics, as well as creating experiential learning opportunities. A detailed analysis of existing training approaches identifies shortcomings and proposes concrete solutions for developing analytical abilities required in the AI-enhanced marketing world.

Research [24] focuses on shedding light on the effects of digital entrepreneurship education (DEE) on how university students in developing nations perceive digital entrepreneurship intention (DEI), attitude (ATT), subjective norms (SNs), perceived behavioral control (PBC), and personal innovativeness (PI). These findings might be used to develop plans and actions that will increase DEE support and advancement.

### **Research gap**

An entrepreneur might possess the abilities and motivation to start a company, but deciding to sell is a critical first step. Products may find out requirements for existence that they can meet through market research with the assistance of a marketing business or independent researcher. Even if an entrepreneur sees a particular market sector, it might investigate the most effective approach to reach that market. To develop a marketing strategy, they may either do it themselves or employ an expert. An accurate budget might assist an entrepreneur in staying prepared for the unexpected nature of running a business. One possible approach could be to prioritize

efficient marketing strategies and allocate the remaining funds based on specific needs. Entrepreneurs can prepare for changes by managing their finances and identifying which expenses are essential. By addressing challenges like competitiveness, time management, juggling work and life, managing people, and a lack of funding, entrepreneurs may use the proposed FPO-GLSTM strategy to overcome failures and hurdles and achieve long-term development and success.

### 3. Proposed method

The section mainly describes the four phases of the proposed algorithm. Initially, data collection utilizing biosensors to obtain important data, followed by data preprocessing using min-max normalization to scale the data to a range, that enhances model performance. The DWT is used to extract feature information from the signal. Finally, the proposed model uses an FPO-GLSTM that improves prediction accuracy by optimizing feature learning and temporal data processing. **Figure 1** shows the framework of the suggested model.

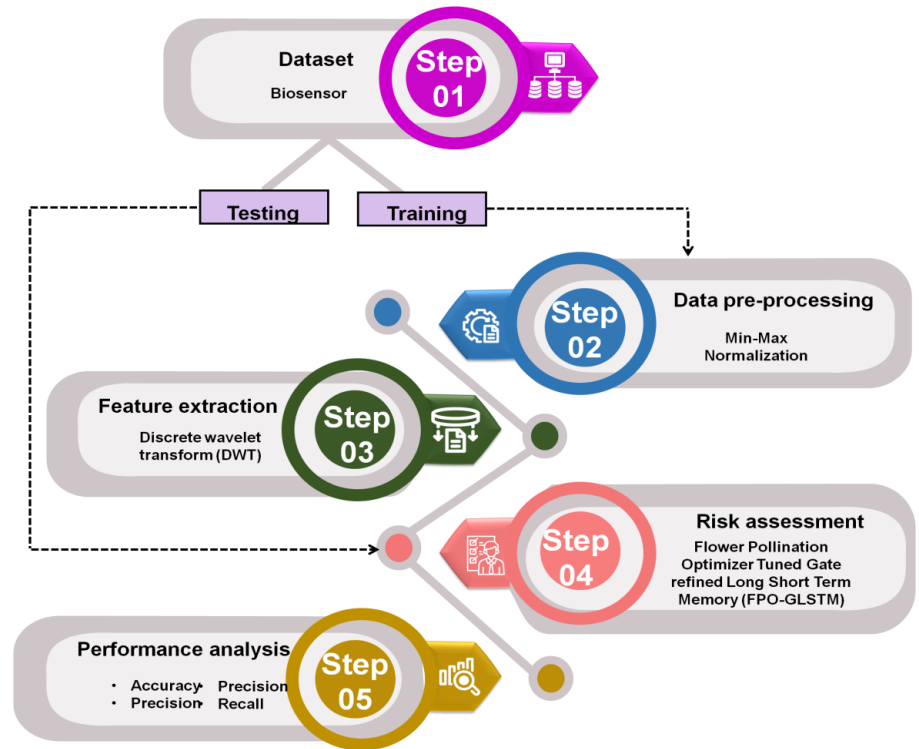


**Figure 1.** Flow of proposed model.

#### 3.1. Dataset

The study dataset is physiological data from college students gathered from Kaggle [25]. This dataset focuses on health risk assessment in high-stress situations, such as academic and entrepreneurial settings, by simulating physiological, psychological, and academic data for college students. It includes variables such as heart rate, blood pressure, cortisol levels, academic performance, and stress responses, aiming to provide a comprehensive view of the factors contributing to stress-related health risks. It is intended to aid in the creation and evaluation of machine learning

models that forecast hazards to occupational health, including physical strain and stress, with potential applications in stress management and intervention strategies.

### 3.2. Data pre-processing using min-max normalization

To enable thorough comparison and evaluation, the original data is standardized to guarantee that the indicators are the same size. Outlier normalization, also known as minimum-maximum normalization, is a linear transformation of the original data that guarantees the output values are scaled between 0 and 1. It decided to use the min-max normalization approach. It works better with data whose values are significantly near to one another. Equation (1) is the transformation function used in the min-max normalization investigation.

$$y' = \frac{y - y(\min)}{y(\max) - y(\min)} \quad (1)$$

where,  $y(\max)$  symbolizes every sample data's greatest value, and  $y(\min)$  symbolizes the sample data's lowest value.

### 3.3. Feature extraction using Discrete Wavelet Transform (DWT)

It is a wavelet transform (WT) that separates the host signal into discontinuous wavelets. Its temporal resolution distinguishes it from the Fourier transform (FT) since it contains more information in both time and frequency. Discrete approaches are necessary for automated WT implementation. The wavelet's most frequent discretization is the dyadic discretization, defined as follows in Equation (2).

$$\psi_{(i,l)}(s) = \frac{1}{\sqrt{2^i}} \psi\left(\frac{s - 2^i l}{2^i}\right) \quad (2)$$

In this case,  $b = 2^i$  and  $a = 2^i l$ . Under certain conditions, Equations (3) and (4) is used to represent the original time function as an orthonormal basis of  $K^2Q$ .

$$e(s) = \sum_{i=-\infty}^{\infty} \sum_{l=-\infty}^{\infty} D_{i,l} \psi_{(i,l)}(s) \quad (3)$$

$$D_{i,l} = \int_{-\infty}^{\infty} e(s) \psi_{(i,l)}^*(s) dt \quad (4)$$

where, the wavelet coefficient is  $D_{i,l}$ . To derive the orthonormal basis of  $\phi(s)$ , multi-resolution approximations are used to generate a second set of basis functions  $\psi(s)$ , as in Equation (5).

$$\phi_{(i,l)}(s) = \frac{1}{\sqrt{2^i}} \phi\left(\frac{s - 2^i l}{2^i}\right) \quad (5)$$

The initial time function may be expressed as Equation (6).

$$c_{i,l} = \int_{-\infty}^{\infty} e(s) \phi_{(i,l)}^*(s) dt \quad (6)$$

The scaling coefficients  $c_{i,l}$  indicate  $i^{th}$  resolution discretization of  $e(s)$ , whereas  $c_{0,l}$  represents the sampled version of  $e(s)$ . Scalability and wavelet values are possibly obtained iteratively at resolutions greater than  $i$  using Equations (7) and (8).

$$c_{i+1,l} = \sum_{j=-\infty}^{\infty} g(j-2l) c_{i,l} \quad (7)$$

$$d_{i+1,l} = \sum_{j=-\infty}^{\infty} h(j-2l) c_{i,l} \quad (8)$$

The initial wavelet used for analysis,  $\psi(s)$  is the source of the low pass and high pass filters,  $g$  and  $h$ . Every distribution of gradually higher frequencies is represented by the wavelet coefficients  $c_{i,l}$ , while the scaling coefficients  $c_{i,l}$  represent the original signal's lower frequency approximations. In the inverse DWT, the input signal  $c_{0,l}$  is represented as a difference series in terms of the wavelet coefficients  $c_{i,l}$ , and the filters  $g$  and  $h$ , as follows in Equation (9).

$$c_{i,l} = \sum_{j=-\infty}^{\infty} h(l-2k) c_{i,l,j} + \sum_{j=-\infty}^{\infty} h(l-2j) d_{i+1,j} \quad (9)$$

The wavelet analysis's quality is determined by the wavelet filters used. Because of its small support in the time area, orthogonality, and ease of computing, it uses the system of wavelets. It selected the following Equation (10).

$$g(0) = 1/\sqrt{2}, \quad g(1) = 1/\sqrt{2}, \quad h(0) = g(1) \quad h(1) = -g(0) \quad (10)$$

The discretization of the input signal  $e(s)$  into  $N$  samples allows Equation (7) to be expressed as a matrix.

$$S_M = \begin{pmatrix} g(0) & g(1) & 0 & \cdot & \cdot \\ h(0) & h(1) & 0 & \cdot & \cdot \\ 0 & g(0) & g(1) & 0 & \cdot \\ 0 & h(0) & h(1) & 0 & \cdot \\ \cdot & \cdot & 0 & \cdot & \cdot \\ \cdot & \cdot & 0 & g(0) & g(1) \\ g(1) & 0 & \cdot & h(0) & h(1) \\ h(1) & 0 & \cdot & 0 & g(0) \\ & & & 0 & h(0) \end{pmatrix} \quad (11)$$

Applying the  $M/2^i WM/2^i$  matrix  $S_{M/2^i}$  to the scaling coefficients of the  $j^{th}$  order  $c_{i+1,l}$  ( $l = 1 \sim \frac{M}{2^{i+1}}$ )  $c_{i+1,l}(i+1)$  yields the scaling coefficients  $c_{i,l}$  ( $l = 1 \sim M/2^i$ ) and the wavelet coefficients  $d_{i+1,l}$  of the  $(i+1)^{th}$  charge resolution. The wavelet coefficients are derived following the  $j-1$  iteration of Equation (11) when the number of data points is  $M = 2^j$ . Dilation, also known as the scale parameter, is a function of size, As seen in **Figure 2**, translation is the location variation of the chosen wavelet along a time axis.

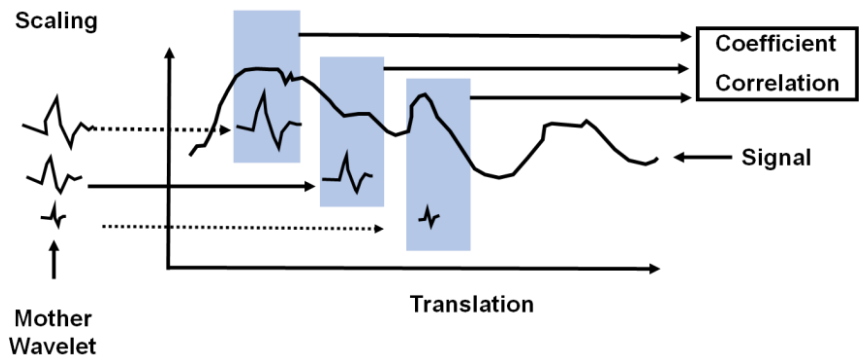


**Figure 2.** Execution of wavelet transforms for signal processing and analysis.

### 3.4. Risk assessment using Flower Pollination Optimizer Tuned Gate refined Long Short Term Memory (FPO-GLSTM)

A hybrid strategy for more accurate health issue monitoring and forecasting is the FPO-GLSTM technique. More accurate predictions for potential health trends and anomalies are rendered possible by the model's improved ability to capture intricate temporal patterns in health data through the use of FPO to adjust the gates inside the GLSTM. The hybrid model is a useful tool for proactive healthcare monitoring and choices, as it excels at managing large, dynamic datasets.

#### 3.4.1. Gate-refined Long Short Term Memory (GLSTM)

Weight sizes largely determine the temporal variations of the error-incorporated signal, BP with real-time recurrent learning or time is likely to cause the error-incorporated signals that run backward in time to either disappear or explode. When it blows up, the weights are likely to begin oscillating, and when it disappears, either the time needed to learn how to bridge greater time gaps is too long, or worse, it doesn't function. To improve the present systems and get beyond the error BP problems mentioned above, a unique kind of recurrent neural network (RNN) is needed. Cells and input/output gates made up the original iteration of this GLSTM method. While avoiding the loss of short-time break capabilities, this technique can bridge time breaks longer than steps, even when the input sequences are noisy or incompressible.

- Structure of LSTM

The following diagram illustrates the four neural networks and other memory units, often known as cells that comprise the GLSTM structure. The information held in cells is altered by the gates. Three different kinds of gates exist.

- Forget gate

The forget gate removes unnecessary information from cells. By multiplying the weighted matrices and adding bias, the inputs at a given time,  $xt$ , and output of the preceding cell,  $ht - 1$ , are calculated. After passing through an activation function, the outcome is a binary output. After that, if the output is 1, the data in the cell state is retained, and if it is 0, the data is discarded.

- Input gate

In a cell state, it carries out the task of adding essential information.

The values that should be kept are filtered after the data is processed using a sigmoid function. In the following step, a vector is created using the function  $\tanh$ ,



which produces an output with all possible values from  $g_{s-1}$  and  $w_s$  that range from  $-1$  to  $+1$ . Finally, to obtain meaningful results, the sigmoid function filtered results, and vector values are multiplied.

- Output gate

It defines the output using the information that is currently stored in the cell state. Using the function  $\tanh$  for cell values, a vector is first created. The following stage is selecting the values that should be kept and regulating the data using the sigmoid function. The final output is the product of the vector and controlled values that serve as the input for the following **Figure 3**.

Considering the first decision to remove unnecessary information from the cell state is crucial. Such decisions are made by the forget gate layer of the sigmoid layers. Where,  $w_s$  and  $g_{s-1}$  are taken into account while making decisions, and the results for any number in cell  $g_{s-1}$  is any value between 0 and 1. If the outcome is 1, 0 indicates that the information must be retained, it means that the data must be thrown away, as in the following Equation (12).

$$e_s = \sigma(X_e \times [g_{s-1}, w_s] + w_s) \quad (12)$$

The next stage is to develop a plan for the information that will be stored in the cells. This procedure is divided into two phases. First, a sigmoid coat layer is part of the input gate layer that resolves the values that need to be updated. Second, a vector of an additional character  $s$  is generated under this scenario by a  $\tanh$  layer intended for addition, as in the following Equations (13) and (14).

$$j_s = \sigma(X_e \times [g_{s-1}, w_s] + a_d) \quad (13)$$

$$D_s = \tanh(X_e \times [g_{s-1}, w_s] + a_d) \quad (14)$$

This stage involves implementation following the completion of all planning and decision-making. It updates to cell state  $d_{s-1}$ . As previously anticipated, to forget the information,  $e_s$  is multiplied by the prior state, and then  $(j_s \times \tilde{D}_s)$  is added. Based on the decision to update the cell state value, the resulting value represents the new character, scaled by a limit, as shown in Equation (15).

$$D_s = e_s \tilde{d}_{s-1}^x + j_s \times D_s \quad (15)$$

Though it will be a filtered output, it is crucial to design the output, which is determined by the cell state. Therefore, part of the cell state that must be shown as the output is selected first by a sigmoid layer. To get the precise output that was determined, the state of this cell is sent along  $\tanh$  and it can be enhanced by adding to the result of the sigmoid gate layer, as in the following Equations (16) and (17).

$$p_s = \sigma(X_p [g_{s-1}, w_s] + a_p) \quad (16)$$

$$g_s = p_s \times \tanh(D_s) \quad (17)$$

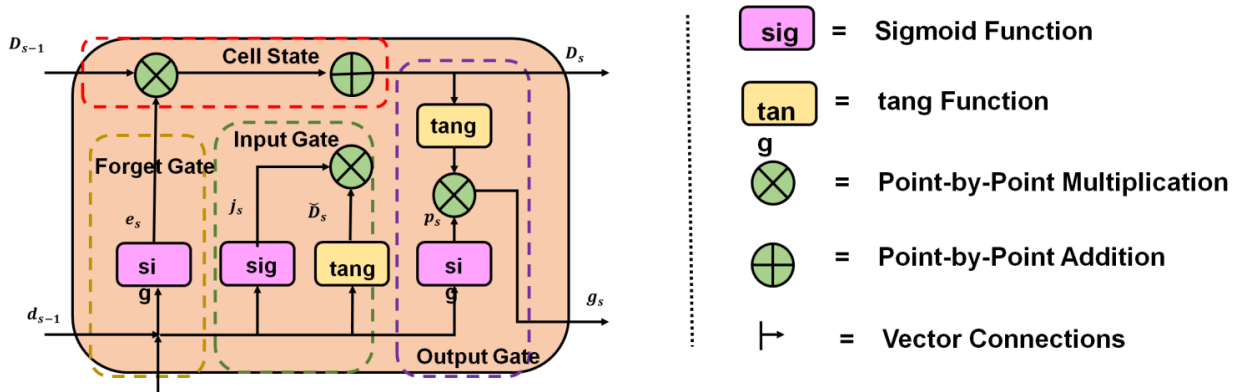


**Figure 3.** Structure of the GLSTM model and key components and data flow.

### 3.4.2. Flower Pollination Optimizer (FPO)

The following assumptions underlie the FPO, flower development rate applies to pollination rate, physical variables, including flower distance and wind speed, examine the difference between global and local pollination; biological allogamy involves a pollinator flying on Levy to achieve a global pollination effect; self-pollinating invitation is a mechanism of area pollination. Every conversion probability serves as the algorithm's representation of this conversion. Below is a description of the FPO's primary steps. The conversion probability parameter  $C$ , the number of floral populations  $N$ , and a random integer  $\text{rand} \in (0,1)$  in FPO are all initialized, as well as evaluating each solution's fitness levels to get the global best solution. Equation (18) is used to implement the transboundary process and update the solution if the conversion rate is  $c > \text{rand}$ .

$$v_j^{s+1} = v_j^s + K(h^x + v_j^s) \quad (18)$$

where,  $v_j^{s+1}$  and  $v_j^s$  stand for the  $(s+1)^{th}$  and  $(s)^{th}$  production solutions, respectively,  $g$  is a globally optimal solution,  $K$  is the step length generated by the pollen propagator Levyflying,  $K$  follows the value of the Levy distribution is input into Equation (19).

$$K \sim \frac{\lambda \Gamma(\lambda) \sin(\pi\lambda/2)}{\pi t^{1+\lambda}} \quad (19)$$

With  $s \gg s_0 > 0$ ,  $s$  being the step dimension,  $s_0$  is the lowest step dimension,  $\Gamma(\lambda)$  as the typical Gamma function, and  $\lambda = 1.5$  selected, Mantegna's technique is used to create the Levy flight step  $K$ .

Equation (20) is used to execute the transboundary process and update the solution if the conversion rate is  $p \leq \text{rand}$ .

$$v_j^{s+1} = v_j^s + \gamma(v_j^s + v_r^s) \quad (20)$$

In this case,  $v_j^s$  and  $v_r^s$  are pollen from explodes of the same plant species, and  $\gamma$  is a random number on  $[0,1]$ . To determine the data processing fitness, compute Steps (3) and (4). Determine if the new solution's fitness approaches the ideal level. Both the response and the fitness are updated. There is no change in the present solution or fitness. The new solution should be designated as the global optimum solution if the global optimal solution's fitness value is greater than the new solution's. The

interaction between pollen individuals, which is readily confined to a local minimum, is the primary determinant of the optimization solution, according to the FPO principle. The issue is fixed by adding the weight of inertia  $\omega$  to the pollen location. As follows in Equation (21), the new position is updated.

$$v_j^{s+1} = \omega \times v_j^s + K(h^x + v_j^s) \quad (21)$$

At the start of every iteration, the risk assessment pollen movement is more strongly impacted by the increased weight of pollen from previous generations in FPO. Additionally, there is less attraction between pollen. The final iteration's lower inertia weight may increase the attraction between pollen. The global search power decreases in this scenario, whereas the local search power increases. Four inertia weights, namely  $\omega_1$ ,  $\omega_2$ ,  $\omega_3$ , and  $\omega_4$ , are chosen to increase FPO to prevent a recurring oscillation close to the extreme location from expanding the moving step size. A constant inertia weight is denoted by  $\omega_1$ , a linear resistance weight by  $\omega_2$ , an exponentially decreasing inertia weight by  $\omega_3$ , and weight of dynamic inertia by  $\omega_4$ . Each weight of inertia is shown using Equations (22)–(25).

$$\omega_1 = 0.7 \quad (22)$$

$$\omega_2 = \omega_{max} - \frac{\omega_{max} - \omega_{min}}{j_{max}} \times j \quad (23)$$

$$\omega_3 = \omega_{min} + (\omega_{max} - \omega_{min})f^{-(4j/j_{max})^2} \quad (24)$$

$$\omega_4 = \omega_{max} - \left(\frac{j}{j_{max}}\right)^3 \times (\omega_{max} - \omega_{min}) \quad (25)$$

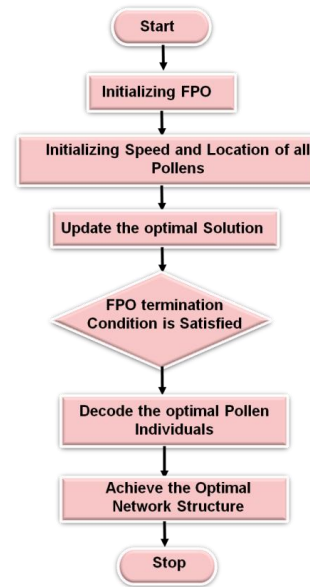


**Figure 4.** Flowchart of the FPO approach.

The number of iterations today is  $j$ ,  $j_{max}$  is the number of iterations at its maximum,  $\omega_{max}$  is the largest inertia weight, and  $\omega_{min}$  is the smallest. The ideal searching effect can find the optimum answer when the inertial weight fluctuates

between 0.9 and 0.4. Therefore, use  $j_{max} = 200$ ,  $\omega_{max} = 0.9$ , and  $\omega_{min} = 0.4$ . **Figure 4** shows the change in four inertial weights as a function of iteration number. The FPO-GLSTM enhances the capacity to modify parameters that lead to more efficient learning and improved management of intricate, non-linear data patterns. It enhanced risk prediction across a range of applications, including environmental monitoring, healthcare, and finance. Algorithm 1 shows the suggested FPO-GLSTM method.

---

**Algorithm 1** FPO-GLSTM

---

```

1: Initialize FPO-GLSTM Parameters
2: Initialize GLSTM
3: for each gate in the GLSTM cell (Forget, Input, Output)
   Calculate gate output using activation functions
4: if Forget gate
   Apply sigmoid to input and previous cell state
   Remove unnecessary data if gate output = 0
5: else if the input gate
   Apply sigmoid and tanh functions to update cell state
6: else if the Output gate
   Calculate output based on the current cell state
   Apply sigmoid for final output
7: end if
8: end for
   Update cell state based on new gate values
   Update hidden state as final output of GLSTM for prediction
9: Initialize FPO for Tuning GLSTM
10: for each flower in population  $N$ 
   Evaluate the fitness of each solution
11: if fitness > current global best solution
   Update global best solution
12: end if
13: end for
14: Main Loop for FPO and GLSTM Integration
15: for each iteration  $j$  in range (1,  $max\_iterations$ )
16: for each flower solution  $v\_j$  in population  $N$ 
   Generate step size  $K$  using the Levy flight formula:
17:  $K = \lambda \Gamma(\lambda) \times \sin(\pi\lambda/2) / (\pi t^{(1+\lambda)})$ 
18: If
   Update  $v\_j^{(s+1)} = v\_j^s + K \times (h \times + v\_j^s)$ 
19: Else
   Select random flower  $v\_r$  from the same species
   Generate random number  $\gamma \in [0,1]$ 
20: end if
21: if using a constant weight
   a)  $\omega = 0.7$ 
22: else if using linear resistance weight
23:  $\omega = \omega_{max} - ((\omega_{max} - \omega_{min})/j_{max}) \times j$ 
24: else if using exponentially decreasing inertia weight
    $\omega = \omega_{min} + (\omega_{max} - \omega_{min}) \times \exp(-((4j/j_{max})^2))$ 
25: else if using dynamic inertia weight
   a)  $\omega = \omega_{max} - ((j/j_{max})^3) \times (\omega_{max} - \omega_{min})$ 
   Evaluate fitness of  $v\_j^{(s+1)}$ 
26: if fitness > current global best solution
   SET global best solution =  $v\_j^{(s+1)}$ 
27: end if
28:
29: end for

```

---

## 4. Result and discussion

The section, briefly explains the experimental setup, evaluation metrics, and study discussion, and the FPO-GLSTM framework and existing benchmarks are thoroughly compared.

### 4.1. Experimental setup

A system with the following configurations was used for the experiment: HP, Windows 10 Pro 64-bit as the operating system (OS), The Intel(R) Core (TM) i7-6700 CPU has 4096 MB of RAM and a 3.40 GHz (8 CPUs) CPU. To enhance data analysis, a variety of Python 3.10 software packages, including Pandas, Imblearn, and Numpy framework, are utilized.

### 4.2. Comparative analysis

Loss and accuracy: The following models and data sets were trained independently using health risk assessment. The term epoch in this case denotes the number of training rounds needed to converge to a patience threshold of five. The original FPO-GLSTM architecture was selected for the work. After more investigation, it was discovered that its efficacy was inadequate, as **Figure 5** shows **Figure 5a** accuracy, and **Figure 5b** loss. Only 90.12% of the data were accurate, representing a loss of 0.2189.

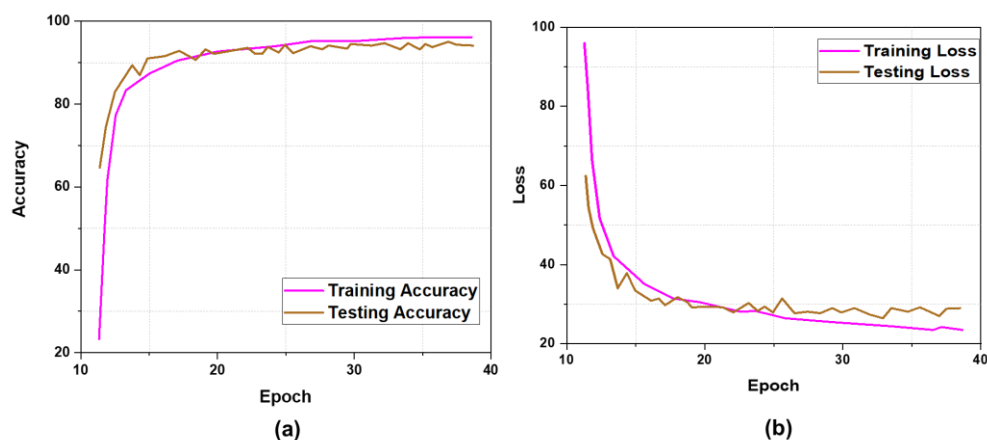


**Figure 5.** Training and testing in the proposed model, (a) accuracy; (b) loss.

Confusion matrix: The classification accuracy of the method for key-event detection using the CM as described in the previous experiment. The technique's rate of misclassification is examined using the confusion matrix. It used the CM to look at the number of enthusiastic framesets that were mistakenly identified as non-excited (false negatives) and the quantity of non-excited framesets that were mistakenly identified as excited (false positives), such as high, low, and moderate. As shown in **Figure 6**, the system performs exceptionally well in classifying activity-related activities.

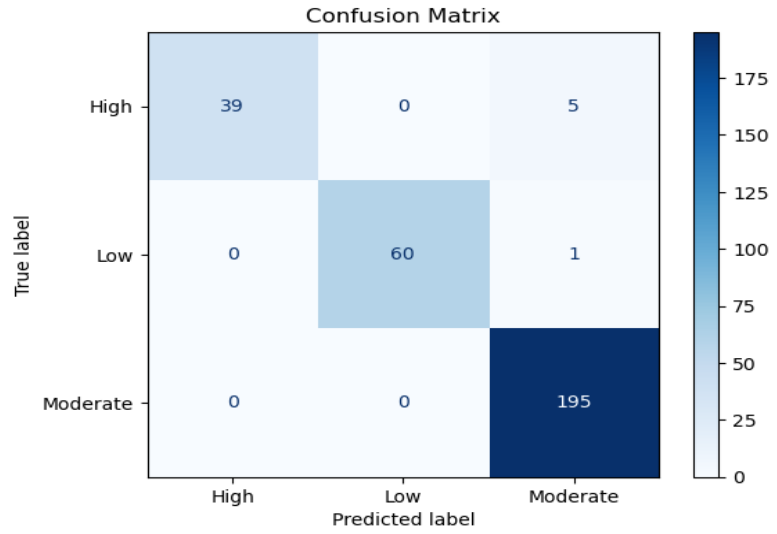


**Figure 6.** Confusion matrix for model evaluation.

The following criteria were used to evaluate the accuracy, precision, recall, and F1-score of the classifier FPO-GLSTM model, as in Equations (25–28).

True positive (TP): It predicts a positive outcome and expects the supplied input to be positive.

False positive (FP): It forecasts as positive despite the input is predicted to be negative.

False negative (FN): It anticipates a negative input and now makes a positive prediction.

True negative (TN): Both the expected and predicted outputs are negative for the given input.

**Table 1** shows the outcome of the proposed FPO-GLSTM method.

**Table 1.** Outcomes of the proposed model.

Gender	Accuracy (%)	Precision (%)	Recall (%)	F1-score (%)
Female	90.36	85.35	89.41	86.65
Male	88.15	83.24	87.20	84.32

Accuracy: A common metric for evaluating how well a model predicts outcomes. It displays the percentage of cases that were successfully classified relative to all instances. While high accuracy suggests a dependable model, it may not offer an exhaustive overview of its performance owing to class imbalance or different factors. **Figure 7** shows the comparison of accuracy in the suggested method. The proposed method EGO-DSVM achieved higher assessment performance, such as female (90.36%), and male (88.15%).

$$\text{Accuracy} = \frac{\text{TP} + \text{TN}}{\text{FP} + \text{FN} + \text{TP} + \text{TN}} \quad (25)$$

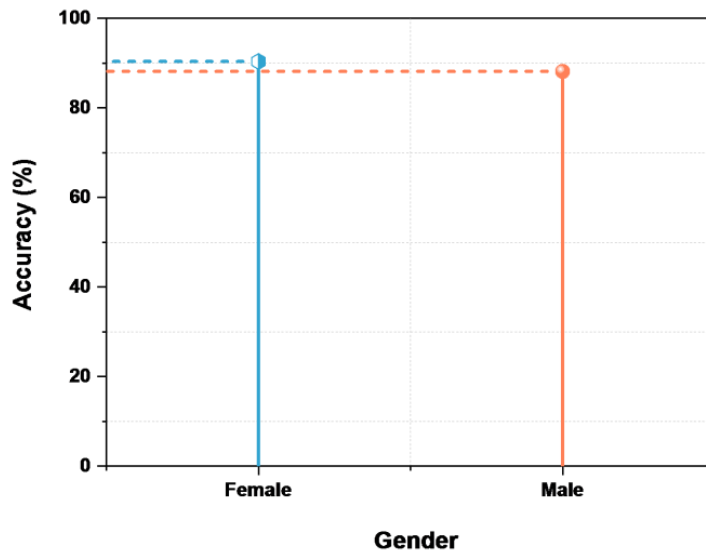


**Figure 7.** Comparative accuracy performance of different models.

Precision: The percentage of accurately predicted positive cases out of all instances anticipated as positive is measured by this statistic. It measures how well the model avoids FP. False alarm rates are lower as precision is higher. **Figure 8** shows the comparison of precision in the suggested method. Health risk assessment of female offer (85.35%), and male (83.24%), respectively.

$$\text{Precision} = \frac{\text{TP}}{\text{FP} + \text{TP}} \quad (26)$$

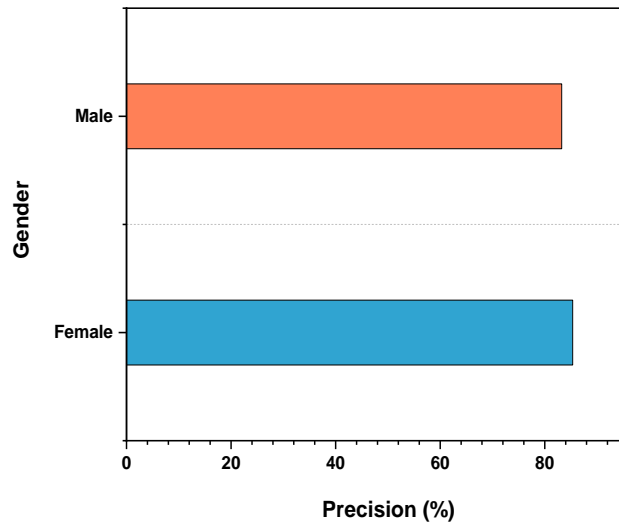


**Figure 8.** Comparative precision performance of different models.

Recall: The model’s ability to identify positive instances is measured as the proportion of TP forecasts to total positive outcomes in the data collection. It evaluates the model’s capacity to recognize every positive example. As recollection increases, FN becomes less frequent. **Figure 9** shows the evaluation performance of recall in the

proposed method. The proposed method outcomes achieved high performance of recall for females (89.41), and males (87.20), respectively.

$$\text{Recall} = \frac{\text{TP}}{\text{TP} + \text{FN}} \quad (27)$$

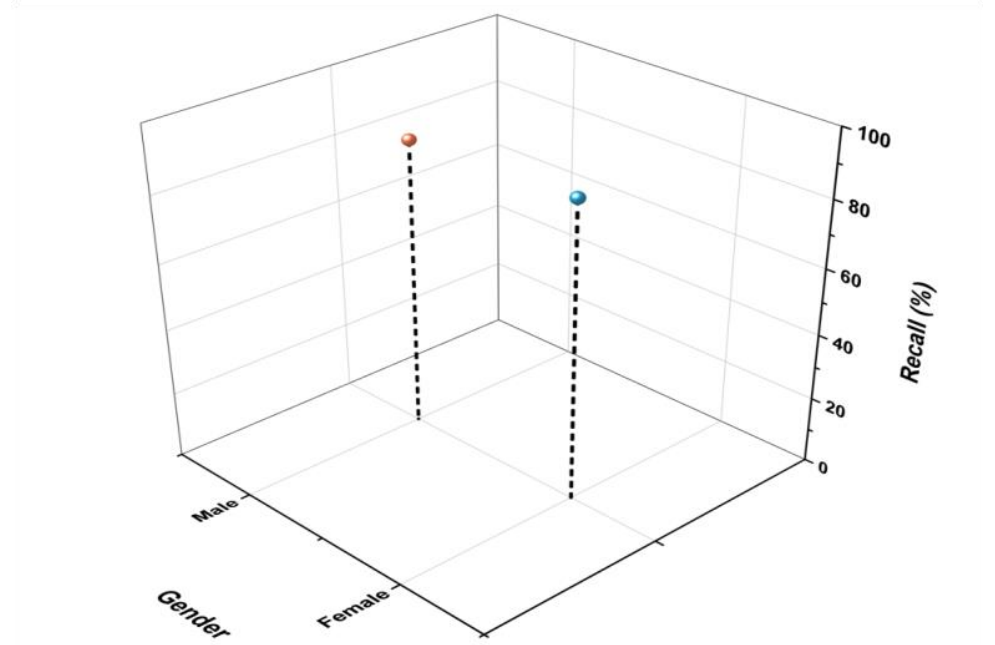


**Figure 9.** Comparative recall performance of different models.

F1-score: Is computed as the accuracy and recall harmonic mean, providing a precise assessment of a model's efficacy. It accounted for both precision and recall values and is helpful in situations that have a class imbalance in the data. The trade-off between recall and precision is better as the F1-score is greater. The experimental results are demonstrated in **Figure 10**. It is shown males and females can achieve the highest F1-score of 86.65% and 84.32%.

$$\text{F1 - score} = \frac{2 \times \text{precision} \times \text{recall}}{\text{precision} + \text{recall}} \quad (28)$$



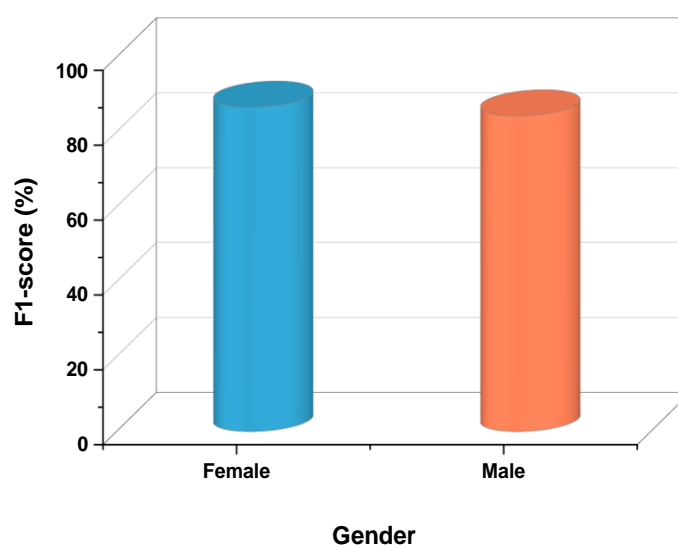


**Figure 10.** Proposed model outcome of F1-score.

### 4.3. Study discussion

The suggested article employs a DL technique to evaluate entrepreneurial strategies and occupational health risk assessment among college students in biosensors. The suggested FPO-GLSTM model offers enhancements and distinctions from the DL method. The experimental setting of the suggested FPO-GLSTM approach for assessing innovation and entrepreneurship management techniques in higher education may be impacted by several elements. To ensure the validity of findings for assessing innovation and entrepreneurship strategies and occupational health risk assessment in colleges, it's important to study and regulate these variables while creating and performing experiments utilizing student health risk assessment of male and female students. With comparatively fewer function evaluations, it may rapidly converge to the ideal solution and require a small number of parameters to be established. Different lengths of sequences can be processed using GLSTM networks. Because GLSTM may dynamically adapt to sequences of varying durations, unlike fixed-size input structures, they are robust and versatile when processing input data with fluctuating temporal dynamics. The confusion matrix provided additional evidence that the model was effective in reducing misclassifications, particularly erroneous positives and false negatives. According to these findings, the FPO-GLSTM model performs admirably in jobs involving health risk assessment, offering accurate forecasts that are robustly evaluated across a range of indicators. Nevertheless, more improvement could improve its functionality in some situations.

### 5. Conclusion

In the work, developed college student's occupational health risk assessment and entrepreneurial strategies in biosensors. The study presents an FPO-GLSTM model to track and forecast health hazards, including stress and physical strain, using biosensor technologies and AI. With pre-processing using min-max normalization, the DWT was used to accurately extract essential characteristics from the data. The suggested technique, EGO-DSVM, performed well in evaluation, with 90.36% accuracy for

females and 88.15% for males. Precision reached 85.35% for females and 83.24% for males, while recall was 89.41% for females and 87.20% for males. The F1-score for females and males were 84.32% and 86.65%, respectively. Although predicting health risks, the FPO-GLSTM model explained a high degree of accuracy and offered specific risk management improvements. Real-time monitoring and individualized health insights are created by the combination of AI with biosensor data, indicating a significant improvement in the administration of student health risks. The suggested strategy improves performance in risk assessment parameters such as F1-score, recall, precision, and accuracy.

**Funding:** The Industry-Education Cooperative and Collaborative Education Project of the Ministry of Education of China ,2024: Construction of a comprehensive ability training system for teachers of the “Foundations of Entrepreneurship” course in colleges and universities based on the OBE concept (2408193953).

**Ethical approval:** Not applicable.

**Conflict of interest:** The author declares no conflict of interest.

## References

1. Haojie, G., 2022. Innovation and entrepreneurship strategies of teachers and students in financial colleges and universities under the direction of food security. *Frontiers in Psychology*, 13, p.848554.
2. Sankaran, S., Rajasekaran, M.P. and Sivapragasam, C., 2020. Project-based learning novel approach to teaching biosensors and transducers course for engineering students. *Journal of Engineering Education Transformations*, 34(1), pp.61–69.
3. Chang, S.H., Shu, Y., Wang, C.L., Chen, M.Y. and Ho, W.S., 2020. Cyber-entrepreneurship as an innovative orientation: Does positive thinking moderate the relationship between cyber-entrepreneurial self-efficacy and cyber-entrepreneurial intentions in Non-IT students? *Computers in Human Behavior*, 107, p.105975.
4. Jena, R.K., 2020. Measuring the impact of business management Student’s attitude towards entrepreneurship education on entrepreneurial intention: A case study. *Computers in Human Behavior*, 107, p.106275.
5. Boldureanu, G., Ionescu, A.M., Bercu, A.M., Bedrule-Grigoruță, M.V. and Boldureanu, D., 2020. Entrepreneurship education through successful entrepreneurial models in higher education institutions. *Sustainability*, 12(3), p.1267.
6. Liu, Y., 2020. The micro-foundations of global business incubation: Stakeholder engagement and strategic entrepreneurial partnerships. *Technological Forecasting and Social Change*, 161, p.120294.
7. Wardana, L.W., Narmaditya, B.S., Wibowo, A., Mahendra, A.M., Wibowo, N.A., Harwida, G. and Rohman, A.N., 2020. The impact of entrepreneurship education and students’ entrepreneurial mindset: the mediating role of attitude and self-efficacy. *Heliyon*, 6(9).
8. Fassbender, U., Papenbrock, J. and Pilz, M., 2022. Teaching entrepreneurship to life-science students through Problem-Based Learning. *The International Journal of Management Education*, 20(3), p.100685.
9. Oliveira, A.W. and Brown, A.O., 2022. Experiencing the entrepreneurial side of science: undergraduate students pitching science-based businesses. *Entrepreneurship Education*, 5(4), pp.367–397.
10. Thurik, A.R., Audretsch, D.B., Block, J.H., Burke, A., Carree, M.A., Dejardin, M., Rietveld, C.A., Sanders, M., Stephan, U. and Wiklund, J., 2024. The impact of entrepreneurship research on other academic fields. *Small Business Economics*, 62(2), pp.727–751.
11. He, M. and Zhang, J., 2023. Evaluating the innovation and entrepreneurship education in colleges using BP neural network. *Soft Computing*, 27(19), pp.14361–14377.
12. Yu, H., Zhang, R. and Kim, C., 2023. Intelligent analysis system of college students’ employment and entrepreneurship situation: Big data and artificial intelligence-driven approach. *Computers and Electrical Engineering*, 110, p.108823.

13. Ojeda-Beltrán, A., Solano-Barliza, A., Arrubla-Hoyos, W., Ortega, D.D., Cama-Pinto, D., Holgado-Terriza, J.A., Damas, M., Toscano-Vanegas, G. and Cama-Pinto, A., 2023. Characterization of Youth Entrepreneurship in Medellín-Colombia Using Machine Learning. *Sustainability*, 15(13), p.10297.
14. Lu, Q., Chai, Y., Ren, L., Ren, P., Zhou, J. and Lin, C., 2023. Research on quality evaluation of innovation and entrepreneurship education for college students based on random forest algorithm and logistic regression model. *Peerj computer science*, 9, p.e1329.
15. High, P. and Alagic, A., 2023. “Design a Sensor”: Implementation of Entrepreneurial-Minded Learning in Undergraduate General Chemistry. *Journal of Chemical Education*, 100(4), pp.1557–1563.
16. Ebrahimi, P., Dustmohammadloo, H., Kabiri, H., Bouzari, P. and Fekete-Farkas, M., 2023. Transformational Entrepreneurship and Digital Platforms: A Combination of ISM-MICMAC and Unsupervised Machine Learning Algorithms. *Big Data and Cognitive Computing*, 7(2), p.118.
17. Schade, P. and Schuhmacher, M.C., 2023. Predicting entrepreneurial activity using machine learning. *Journal of Business Venturing Insights*, 19, p.e00357.
18. Bell, R., 2021. Underpinning the entrepreneurship educator’s toolkit: Conceptualising the influence of educational philosophies and theory. *Entrepreneurship Education*, 4(1), pp.1–18.
19. Bonsaksen, T., Magne, T.A., Stigen, L., Gramstad, A., Åsli, L., Mørk, G., Johnson, S.G. and Carstensen, T., 2021. Associations between occupational therapy students’ academic performance and their study approaches and perceptions of the learning environment. *BMC Medical Education*, 21, pp.1–8.
20. Kakkar, S., Kwapinski, W., Howard, C.A., and Kumar, K.V., 2021. Deep neural networks in chemical engineering classrooms to accurately model adsorption equilibrium data. *Education for Chemical Engineers*, 36, pp.115–127.
21. Verdugo, G.B. and Villarroel, A.V., 2021. Measuring the association between students’ exposure to social media and their valuation of sustainability in entrepreneurship. *Heliyon*, 7(6).
22. Pan, S., Hafez, B., Iskandar, A. and Ming, Z., 2024. Integrating constructivist principles in an adaptive hybrid learning system for developing social entrepreneurship education among college students. *Learning and Motivation*, 87, p.102023.
23. Allil, K., 2024. Integrating AI-driven marketing analytics techniques into the classroom: pedagogical strategies for enhancing student engagement and future business success. *Journal of Marketing Analytics*, pp.1–27.
24. Nguyen, P.N.D. and Nguyen, H.H., 2024. Unveiling the link between digital entrepreneurship education and intention among university students in an emerging economy. *Technological Forecasting and Social Change*, 203, p.123330.
25. <https://www.kaggle.com/datasets/ziya07/student-health-data>